

**The Molecular Role of Taurine in the Protection Against Obesity and Metabolic Diseases**

**A Thesis**

**Presented to the Faculty of the Graduate School  
of Cornell University**

**In Partial Fulfillment of the Requirements for the Degree of  
Master of Nutrition Sciences**

**by**

**Pei-Yin Tsai**

**August 2022**

**Chair: Dr. Joeva Barrow**

**Committee: Dr. Martha Field and Dr. Nathaniel Vacanti**

© 2022[Pei-Yin Tsai]

## ABSTRACT

Taurine has been reported to prevent obesity by influencing thermogenesis. To understand the underlying molecular mechanism of how taurine impacts thermogenesis, we first profiled the taurine biosynthetic pathway under pharmacologically-activated thermogenesis. Based on our study, we found that taurine biosynthetic enzymes, especially ADO, significantly upregulated in inguinal adipocytes in response to thermogenesis. Moreover, the ablation of ADO in adipocytes demonstrated a lower mitochondrial oxygen consumption rate and significantly downregulated taurine level, which suggested that taurine might play a crucial role in regulating healthy mitochondria functions. To understand the large-scale association between taurine and thermogenic adipocytes, we performed an ATAC-seq analysis, which illustrated that taurine supplementation in inguinal cells increased chromatin accessibilities in the hypoxia-inducible factor 1 pathway and glucose metabolic-related genes, suggesting that taurine might regulate mitochondria functions and accelerate the thermogenic-driven metabolism. Further studies are required to analyze whether gene accessibilities can transcribe into proteins and relate to thermogenesis.

## **BIOGRAPHICAL SKETCH**

Pei-Yin Tsai pursued her Bachelor of Science degree in Health and Nutrition at Taipei Medical University, Taiwan. After becoming a dietician, she decided to learn more about metabolism so that one day she can contribute her ability to rescue health problems.

In 2020, Pei-Yin joined the Master's program in Nutrition Sciences at Cornell University. During these two years, she worked with Dr. Joeva Barrow to learn the biology of adipocytes and thermogenesis.

The thesis, *The Molecular Role of Taurine in the Protection Against Obesity and Metabolic Diseases*, was supervised by Dr. Joeva Barrow. After graduating from the Master's program, Pei-Yin decided to pursue a Ph.D. at Cornell University and hopes to become an independent scientist in the future.

## ACKNOWLEDGMENTS

I would like to offer my deepest and sincere gratitude to all those who made my thesis possible.

I appreciate Dr. Joeva Barrow, who served as the chair and guided me for the last two years. I am grateful to her for her patience and endless guidance, which encouraged me to face any challenges and motivated my interest in doing research.

I would like to thank my committee members, Dr. Martha Field and Dr. Nathaniel Vacanti, they gave me endless support and suggestions to help me deal with difficulties and improve my research.

It's my pleasure to have warm lab members and colleagues, I am grateful that Yang Liu, Yue Qu, Kaydine Edward, Siwen Xue, and Chloe Chen gave me company and support during the group meeting.

Thanks to Dr. Paul Soloway, Bo Shui, and Seoyeon Lee for their assistance with the ATAC-seq analysis.

Last but not least, I would like to thank my supportive family, whose encouragement enabled me to overcome obstacles and become determined to pursue my interests.

## Table of Content

### Chapter 1:

- **Introduction** -----P. 1-4

### Chapter 2:

- **Map the Taurine Biosynthesis Pathway in Thermogenic Adipocytes** -----P. 5
- **Experiment Model and Methods** -----P. 5-7
- **Results** -----P. 8-10

### Chapter 3:

- **Quantify the Level and Localization of Taurine in Inguinal adipocytes in Response to NST Activation** -----P. 11
- **Experiment Model and Methods** -----P. 11-12
- **Results** -----P. 13-14

### Chapter 4:

- **Assess the Impact of Taurine on Chromatin Accessibility in Thermogenic Adipocytes** -----P. 15
- **Experiment Model and Methods** -----P. 15-16
- **Results** -----P. 17-18

### Chapter 5:

- **Discussion** -----P. 19-21

### Chapter 6:

- **References** -----P. 22-24

### Chapter 7:

- **Supplementary Data** -----P.25

## Chapter 1

### **Introduction**

As a result of poor dietary eating habits and sedentary lifestyles, the population of individuals who are classified as obese—defined as having a body mass index (BMI) greater than or equal to 30 kg/m<sup>2</sup>, continues to increase annually and is now considered a global pandemic issue. Surprisingly, according to the Dietary Guidelines for Americans 2020-2025, about 74 percent of adults are overweight or obese in the US, and the obesity prevalence has increased from 30.5% to 41.9%. Obesity not only damages people's confidence, but also impacts countries' economic developments by causing a burden on the health care system<sup>1,2</sup>. In addition, over 60 percent of overweight or obese adults have an increased probability of developing comorbidities such as cancer, type 2 diabetes, and even an increased risk of serious illnesses, such as COVID-19-elevated fatality rate<sup>3</sup>. Traditionally, there are several approaches to treat obesity. Current treatment options to combat obesity includes decreasing calorie intake, increasing physical activity, having bariatric surgery, and pharmacotherapy. These treatment options however often have poor long-term efficiency and have serious side effects. For example, surgical intervention options such as bariatric surgery may impact nutrient absorption, or cause other complications, such as acid reflux, nausea, dumping syndrome, or regaining body weight after the approach<sup>4,5</sup>. Due to these side effects and lack of efficiencies in long-term efficacy, patients with obesity have failed to maintain the ideal body weight for long periods. The need therefore to identify another less invasive and novel treatment to prevent obesity is warranted.

One attractive treatment option is to take advantage of the molecular properties of human brown adipose tissue (BAT) and a process known as non-shivering thermogenesis (NST). NST is a molecular pathway that could raise energy expenditure build on specialized brown adipocytes, which differs from shivering thermogenesis depends on muscle activity. In humans, the thermogenic effect of brown fat is negatively correlated with BMI and is associated with an elevation in energy expenditure<sup>6</sup>. NST can be induced and activated by cold acclimation which stimulates the sympathetic nervous system to secrete norepinephrine (Fig. 1-1A)<sup>7</sup>. For example, when volunteers were exposed to a mild cold environment for two hours and given 18F-fluorodeoxyglucose, 18F-fluorodeoxyglucose uptake was significantly increased in the interscapular regions under a positron-emission tomography and computed tomography (PET-CT) scanner, where BAT is mainly localized. Moreover, the resting metabolic rate and the respiratory rate were all increased as a result<sup>8</sup>. Collectively, these data demonstrated that during cold exposure, BAT had to consume more energy substrates to balance the energy expenditure via NST. NST depends on brown adipocytes enriched with specialized

mitochondria that expresses uncoupling protein 1, UCP-1, which is distinct from white adipocytes, that mainly store lipid for excess energy (Fig. 1-1B). UCP-1 is located on the mitochondria's inner membrane. UCP-1 can dissipate hydrogen ions from the mitochondrial intermembrane space into the mitochondria matrix, to generate heat, instead of passing through the ATP synthase (Fig. 1-1C)<sup>9</sup>. UCP-1 is an essential indicator for NST, because UCP-1 knock out mice are unable to produce enough heat to maintain their body temperature<sup>10</sup>. Therefore, mammals need to consume more nutrients to compensate for the loss of energy via the heat production by UCP-1 in order to combat obesity and mitigate risk factors from chronic diseases, such as insulin resistance<sup>11</sup>.

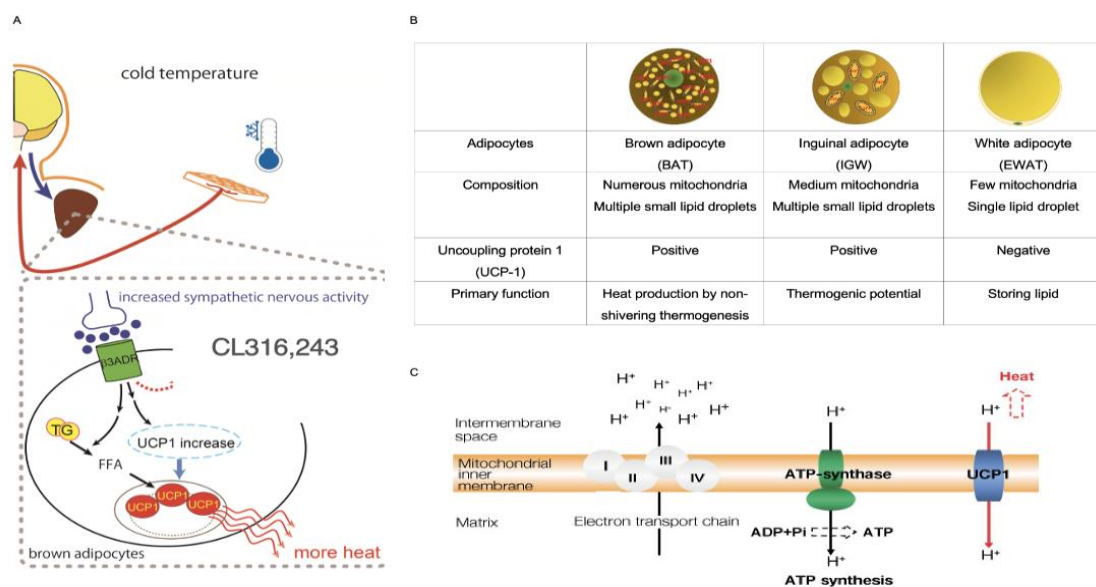


**Figure 1-1 Thermogenic adipocytes and non-shivering thermogenesis (NST).**

(A) Approaches to activate thermogenesis. The figure was adapted from Sun et al., 2016

(B) Overview of the main characteristics among brown (BAT), beige (IGW) and white adipocytes (EWAT). The figure was adapted from Contreras et al., 2017

(C) General overview of NST. NST primarily depends on mitochondria that specialized with UCP-1, which can dissipate the proton gradient in the mitochondrial inner membrane. The figure was from Brondani et al., 2012.

β3ADR: β3 adrenergic receptors; TG: triglyceride; FFA: free fatty acids

In addition to BAT, there is another brown adipose like adipocytes, beige adipocytes, which contains less UCP-1 but could become functionally thermogenic and UCP-1 positive during browning by cold acclimation or pharmacological intervention through activation of the sympathetic nervous system. Beige adipose is a subcutaneous fat in mammals. When mice were injected with CL 316,243, an alternative method to specifically stimulate a beta-3 adrenergic receptor to increase adenylyl cyclase, it elevates the amount of c-AMP as well as cAMP-dependent protein kinase (PKA) to promote lipolysis<sup>12</sup>. As a result, thermogenic transcriptional regulators, peroxisome proliferator activated receptor gamma (PPAR-γ), peroxisome proliferator-activated receptor-gamma coactivator (PGC-1α),

and UCP-1 all increased, illustrating that NST was operating in beige adipocytes<sup>13-15</sup>. Nonetheless, it's not ideal to make people stay in cold environment forever, and there are no safe pharmacological treatments that could active NST. Therefore, scientists are looking for an alternative pathway that could active NST to protect against obesity and metabolic disease.

Intriguingly, in addition to environmental stimulus and pharmacological treatments, researchers have also claimed that some metabolites might have the thermogenic capacity to protect against obesity. An example of a metabolite with this capacity is an amino sulfonic acid, taurine (2-aminoethanesulfonate). Taurine is the most abundant free amino acid in mammalian tissues, and it is often found in animal proteins that are expressed in livers, muscle, and kidney<sup>16</sup>. Numerous studies have elucidated the diverse physiological and biochemical function of taurine. As a supplement, taurine can act as an antioxidant that can decrease inflammation and prevent chronic metabolomic diseases, a valuable supplement for muscle strength to improve physical activity, a bile acid conjugator for synthesizing taurocholic acid to regulate lipid metabolism and a subset of mitochondria tRNA modification<sup>17-20</sup>. In addition, recent and exhaustive evidence demonstrated that taurine has anti-obesity characteristics in adipocytes. Previous research illustrated that the plasma taurine level is negatively correlated with body weight between obese and normal weight participants<sup>21</sup>. In animal study, administrated high-fat diet (HFD) mice with 2 % taurine supplementation for 28 weeks could also decrease body weight and body fat (Fig 1-2A, B)<sup>22</sup>. Additionally, in human studies, it was shown that giving obese people with three grams of taurine supplement for seven weeks can significantly decrease the body weight<sup>23</sup>.

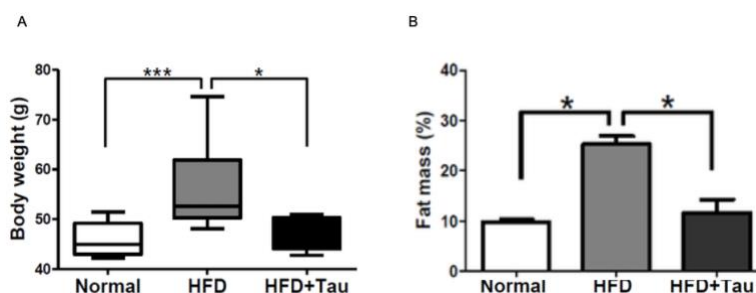


**Figure 1-2 Effect of taurine on body weight loss in high-fat diet**

(A) Body weight of mice fed with normal chew diet, HFD, or HFD + taurine (2% in drinking water) for 28 weeks (n = 10/group).

(B) Fat mass percentage of the mice fed with normal chew diet, HFD, or HFD + taurine (2% in drinking water) for 28 weeks.

It is well-known that obesity elicits chronic inflammation, therefore some research suggests that taurine treatment could down regulate pro-inflammatory markers in obesity-related hypertrophic adipocytes to prevent obesity. For example, taurine could induce the inflammatory M1 macrophage

marker switch to an anti-inflammatory M2 macrophage in order to inhibit the infiltration of immune cells to impede the adipogenesis progression<sup>24,25</sup>. Furthermore, recent studies have shown that taurine could activate thermogenic markers, such as UCP-1 and PGC1- $\alpha$  markers in primary inguinal and white adipocytes. In line with this, mice treated with taurine also had successfully maintained core body temperature during acute cold exposure and increased oxygen consumption<sup>26</sup>. Notably, whether in cold exposure or with CL injection, the amino acid level assessment found that plasma and adipocyte taurine levels increased dramatically<sup>27,28</sup>. In addition, one study also showed that HFD mice treated with taurine would have decreased levels of adipogenesis-related transcription factors such as PPAR- $\alpha$ , PPAR- $\gamma$ , C/EBP- $\alpha$ , C/EBP- $\beta$ , and AP2 in inguinal adipocytes<sup>29</sup>, which demonstrates the negative adipogenesis regulated ability of taurine.

The taurine level in mammals is not only derived from dietary sources, but taurine can also be endogenously derived from cysteine or cysteamine, as well. Firstly, cysteine is oxidized by cysteine dioxygenase (CDO) to synthesize cysteine sulfinic acid, followed by the conversion to hypotaurine by cysteine sulfinic acid decarboxylase (CSAD). Subsequently, hypotaurine is oxidized by hypotaurine dehydrogenase, to synthesize taurine<sup>30</sup>, although, the exact function of hypotaurine dehydrogenase is still unclear. There is an alternative taurine biosynthesis pathway that oxidizes cysteamine by cysteamine dioxygenase (ADO) to generate taurine<sup>31,32</sup>. CDO and ADO belong to the cupin superfamily<sup>33</sup>. CDO was first discovered in rat crude liver tissue in the 1960s<sup>34</sup>, and ADO was described in horse kidneys in 1966<sup>35</sup>. Not including the high amount of taurine in livers and kidneys, scientists found out that the high expression levels of CDO, CSAD and ADO in adipocytes explains the high levels of taurine in adipocytes. Compared with pre-adipocytes, the expression of taurine synthesis enzymes is robustly upregulated in differentiated adipocytes. Of note, established data shows that mRNA expression of CDO decreased in HFD and genetically obese mice<sup>36</sup>, explained the negative correlation between taurine synthesis and obesity. The effect of taurine as an anti-obesity agent is well-known. However, the underlying molecular mechanism of how taurine activates thermogenesis to combat obesity, and whether the phenotype is applied to adipocytes are still enigmatic. Therefore, the first research goal of my study is to identify which adipocytes would mainly contribute to the taurine biosynthesis in response to NST activation. Secondly, I will assess the dynamics of taurine localization in response to thermogenic activation in order to acknowledge how taurine gets metabolized in thermogenic adipocytes. Finally, I will evaluate the large-scale association between taurine and chromatin accessibilities in thermogenic adipocytes in order to identify genomic regions in the chromatin that are regulated by taurine.

## CHAPTER 2

### **Aim 1: Map the taurine biosynthesis pathway in thermogenic adipocytes.**

#### **Research Rationale**

The impact of taurine on the protection of obesity in animals and humans has been well-reported<sup>32,33</sup>. The mechanism, however, of how taurine protects against obesity remains unknown. Some literature suggests that the anti-obesity characteristics of taurine are mediated through the activation of non-shivering thermogenesis (NST)<sup>21</sup>. Brown and beige adipocytes are the main sites of NST and have the ability to synthesize taurine<sup>25</sup> but the details surrounding taurine biosynthesis in these tissues are not known. To address this knowledge gap, my first focus of Aim 1 is to determine which thermogenic adipocytes plays the most dominant role in taurine biosynthesis during thermogenesis. My second focus is to dissect the taurine biosynthesis pathway, because taurine can be synthesized from two distinct biochemical pathways, either using cysteine or cysteamine as substrates<sup>29,30</sup> (Fig. 2-1A). In this aim, I will profile the taurine synthetic pathway to discover the main route of elevated endogenous taurine levels under thermogenesis by assaying the individual taurine biogenesis enzymes in thermogenic adipose depots. After discovering the most dominant taurine biosynthetic enzyme under thermogenesis, I will eliminate this protein in a thermogenic adipocyte cell line to determine if ablation of this enzyme would blunt the taurine synthesis and impair the thermogenic capacity. This will reveal the functional dependency of this taurine biosynthetic enzyme.

#### **Experiment Model and Methods**

##### **Mice**

4-week-old wild-type male C57BL/6J mice were purchased from Jackson Laboratory (#000664), and mice studies were conducted under the approval of the Cornell University Institutional Animal Care and Use Committee. Mice were housed at room temperature (25 °C) with 12-hour dark and light cycles and fed a normal chow diet and water ad libitum. Then, 5-week-old mice were acclimated to a thermoneutral environment (30 °C) for 7 days before the treatment. For pharmacologically-induced thermogenesis experiments, mice were injected daily via intraperitoneal injection (IP) with saline or with 1 mg/kg CL 316,243 (Cayman #17499) (n=5, per treatment) for 7 days. Mice were then euthanized with carbon dioxide. Subsequently, brown, inguinal, and white depots as well as liver tissue were collected and immediately frozen in liquid nitrogen, and stored at -80 °C.

### **Immortalized Cell line**

The brown fat DE 2.3 cell line was plated on polystyrene cell culture plated with gelatin-coating. After 24 hours, cells were differentiated with DMEM/F12 (supplemented with 5 ug/mL insulin, 1 µM Rosiglitazone, 1 µM Dexamethasone, 0.5 mM Isobutylmethylxanthine, and 1 nM T3). After 48 hours, the medium was replaced with maintenance media (5 ug/mL Insulin, 1 µM Rosiglitazone, and 1 nM T3). The medium was replenished every two days until Day 6. On the seventh day, cells were treated with 1uM CL 316,243 or PBS.

### **Crispr Cas9 Cloning**

The sgRNAs of CRISPR-Cas9-based ADO knockout cells were designed using the following database <https://chopchop.cbu.uib.no/>. The guide sequences are as follows: sgADO forward: 5'-*TTCCCGGGCCGAGTACACCG*-3', sgADO reverse: 5'-*CGGTGTACTCGGCCCGGAA*-3'. Guides were then annealed to the LENTICRISPR v2.0 plasmid. Then 1ug of vector CRISPR DNA Plasmid was transfected in 293T cells along with PDM2 (3ug) and PsPAX (4ug) plasmids using the Polyfect reagent. After 48 hours, the lentiviral media was collected from the 293T cells and transduced into the brown fat DE 2.3 cell line. Stable cultures were then generated via puromycin selection (1ug/mL).

### **Immunoblotting and Protein Extraction**

The tissues were lysed with 2% SDS supplemented with protease inhibitors, and then homogenized for 30 minutes at 4°C with metal beads. To isolate protein from cell culture, cells were washed with PBS buffer and then scraped with 2% SDS lysis buffer. Cells were incubated at 4°C for an hour followed by sonication for 10 minutes. Protein isolation was followed by 15 minutes of centrifugation. The supernatant was then removed, and the protein concentration was determined by Pierce™ BCA Protein Assay Kit (Thermo Fisher #23227). A protein sample was mixed with 4x laemmli blue and resolved on 12% SDS-polyacrylamide gels, followed by transfer to polyvinylidene fluoride (PVDF) membranes. After blocking the membranes with 5% milk for an hour, they were washed with TBST and then incubated with primary antibodies as Actin (Cell signaling #4967), CDO (Abcam #196593), CSAD (Thermo Fisher #PA5-120240), ADO (Thermo Fisher #PA5-78733), UCP1 (Abcam #209483) overnight, and then targeted by secondary anti-mouse or anti-rabbit antibody. The membranes were imaged by FluorChem system. Densitometry was performed using the AlphaView software.

### **RNA Isolation and Real-Time Quantitative RT-PCR**

Tissue or cells were homogenized with a Qiagen TissueLyser II in Trizol, followed by mixing with chloroform to extract total RNA. The samples were precipitated and purified using isopropanol, and

75% ethanol, respectively. Reverse transcription of cDNA concentration was quantified by Nanodrop and performed using qScript cDNA Synthesis kit (Quanta Bio #95161500). In this study, real-time qPCR was performed with the CFX384 Real-Time PCR System using SYBR Green.

### **Taurine Measurement**

Differentiated DE 2.3 cells were treated with 1 $\mu$ M CL 316,243 for 24 hours and then processed as cell lysate. Subsequently, the taurine concentration was measured by the taurine assay kit (Cell Biolab # MET-5071)

### **Mitochondria Isolation and Seahorse**

The cells were washed with PBS and scraped with isolation buffer (300mM sucrose, 5mM HEPES, 1mM EDTA, pH 7.2 with KOH). Cells were transferred into a pre-chilled glass-Teflon homogenizer and stroked 13 times to lyse the cells. The cell lysate was resuspended and transferred into a 2mL tube, then centrifuged for 10 minutes at 800 g at 4°C. The supernatant was collected and spun it for 10 minutes at 8500 g at 4°C to pellet the mitochondria. We then washed the mitochondria with 1x MAS buffer (70mM sucrose, 220mM mannitol, 5mM KH<sub>2</sub>PO<sub>4</sub>, 5mM MgCl, 2mM HEPES, 1mM EGTA, pH7.2 with KOH) and centrifuged for further 10 minutes at 8500 g at 4°C. After removing the supernatant, the mitochondria pellet was resuspended with 100  $\mu$ L MAS buffer and quantified by BCA. For measuring the mitochondrial OCR value via seahorse, we seeded 10 $\mu$ g/ $\mu$ L of mitochondria into XFe24 cell culture plates and spun at 2000g at 4°C for 20 minutes, followed by carefully adding 450  $\mu$ L cold MAS buffer into each well. The mitochondrial stress test compounds were as follows (final concentration): A: Pyruvate (9 mM) and Malic acid (9 mM) (for pyruvate-driven respiration), B: Oligomycin (1.5  $\mu$ M), C: FCCP (20  $\mu$ M), D: Rotenone/Antimycin A (135  $\mu$ M each). Respirometry data were collected using the Agilent Wave software v2.4.

### **Quantification and Statistical Analysis**

All data were expressed as mean  $\pm$  SEM unless otherwise annotated. Two-tailed unpaired Student's t-test and multiple t-test were performed to determine the difference between the two independent groups. GraphPad Prism 9 was used for statistical analysis. The significance level was considered at  $p < 0.05$ . The value of n and the statistical parameters are illustrated in each figure legend.

## **Results**

**The taurine biosynthesis enzyme ADO is the most responsive to thermogenic activation.** To examine the response of the taurine biosynthetic enzymes to pharmacologically-activated thermogenesis, mice were injected with the  $\beta$ 3 receptor agonist CL 316, 243, or saline for seven days (Fig. 2-1B). We then extracted the three main adipose depots: brown adipose tissue (BAT), inguinal adipose tissue (IGW), and white adipose tissue (WAT) to profile the taurine biosynthetic enzymes expression. As can be seen in immunoblotting, the thermogenic marker, UCP-1, strongly increased in all three types of adipose pads compared to the saline groups, demonstrating that thermogenesis has been successfully activated (Fig. 2-1 C-E). We also observed a significant elevation of taurine biosynthetic enzymes CDO, CSAD, and ADO only in the IGW depots, compared to BAT and EWAT indicating that IGW plays the most dominant role in regulating taurine biosynthesis under thermogenesis. Of the three main taurine biosynthetic enzymes, the quantification analysis demonstrated that ADO protein levels were the most significantly upregulated in the IGW tissue (Figure 2-1 F-H). We also measured mRNA levels following thermogenic activation and the UCP-1 mRNA expression was upregulated in all three types of adipose depots compared to the saline control group again indicating that we successfully activated the thermogenesis program (Figure 2-1 I-K). Though the CDO and CSAD mRNA expression increased in EWAT, they did not transcribe into protein expression. Interestingly, the relative mRNA level of taurine biosynthetic enzymes did not change in BAT, but was upregulated in IGW depots corresponding to the increases in protein expression. To determine if the increase in ADO mRNA and protein levels is specific to the response of activated thermogenesis, we also tested the protein and mRNA expressions in the liver which also expresses taurine biosynthetic enzymes. There were no significant changes in ADO levels in the liver indicating that the increased level of ADO is specific to IGW, not a global body effect (Fig. 2-1 L-N). Together, our results demonstrated that the elevated taurine biosynthetic protein expression was specific to thermogenic inguinal adipocytes in response to the adrenergic signaling, and among the three enzymes, the ADO is the most responsive to the pharmacologically-activated thermogenesis.

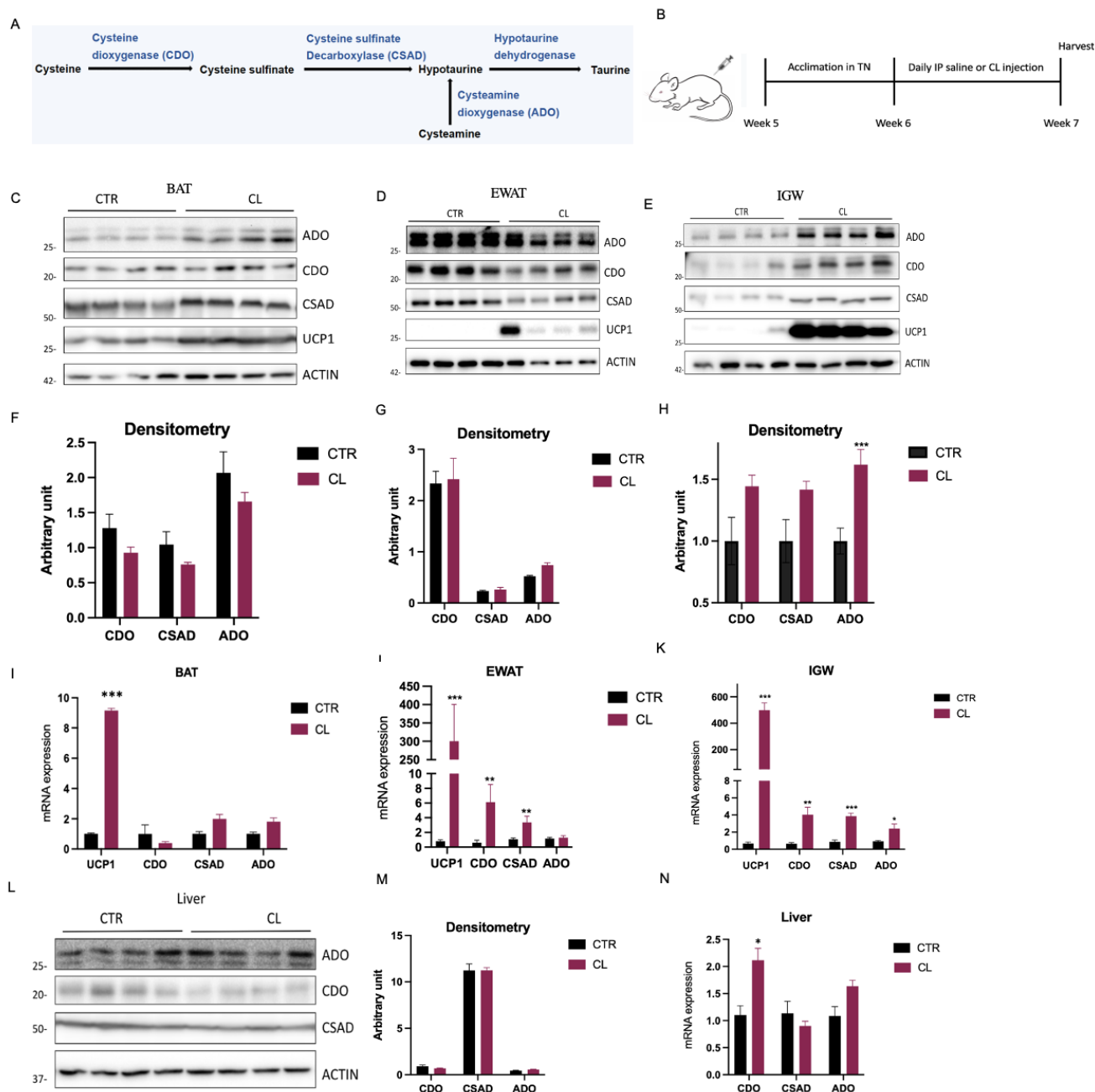


**Figure 2-1. ADO expression is highly enriched in inguinal adipose tissues (IGW) during adrenergic stimulation**

(A) The scheme of the taurine biosynthetic pathway

(B) The scheme of the pharmacologically-activated thermogenesis experiment. Five-week-old mice had been acclimated in thermoneutral environment (TN, 30 °C) for 1 week and had an intraperitoneal injection with saline or CL 316, 243 for seven days (n=4)

(C-E) Representative immunoblotting of taurine biosynthetic enzymes and thermogenic marker, UCP1, in brown, inguinal, and white adipose tissues from six-week-old mice with actin as the protein loading control

(F-H) Protein quantification level of taurine biosynthetic enzymes in BAT, EWAT and IGW, respectively.

(I-K) Relative mRNA expression of thermogenic marker, UCP1 and taurine biosynthetic enzymes among three adipocytes

(L) Representative immunoblotting of taurine biosynthetic enzymes in the liver with actin as the loading control

(M) Immunoblotting of ADO-KO mitochondria protein expression with VDAC as the loading control

(N) Relative mRNA expression of taurine biosynthetic enzymes in the liver

All figures and data are represented as mean  $\pm$  SEM. \* $p < 0.05$ , \*\* $p < 0.01$ , \*\*\* $p < 0.001$  by Student's t test

**ADO ablation blunts the taurine production and mitochondrial respiration capacity in thermogenic adipocytes.** Based on our previous results demonstrating the increase of ADO protein levels in IGW depots in response to activated thermogenesis, it suggests that the ADO biosynthetic pathway may be the dominate pathway for taurine biosynthesis in this depot (Fig. 2-1H). Thus, we investigated whether the lack of ADO would blunt the biological thermogenic function of adipocytes. To generate the loss-of-function model, we knocked out the ADO via the CRISPR Cas9 system in an immortalized adipose cell line, DE 2.3. The immunoblotting illustrated the successful knock-out of ADO at the protein level (Fig. 2-2A), which is consistent with the significantly decreased level of ADO in mRNA expression (Fig. 2-2B). Wondering if the loss of ADO would blunt the taurine biosynthesis, we quantified the taurine level under CL treatment. Compared to the CTR, ADO-KO adipocytes decreased endogenous taurine synthesis (Fig. 2-2C). We then investigated if the loss-of-ADO would impede the biological function of thermogenic adipocytes by deteriorating the mitochondrial respiratory capacity. To amplify the mitochondria signals, we isolated the mitochondria from the ADO-KO and control adipocytes (Fig. 2-2D). There were no differences in the UCP-1 and electron transport chain protein complexes (Fig. 2-2E). We next measured the oxygen consumption rate of the ADO-KO from isolated mitochondria via Seahorse. Intriguingly, ablation of ADO can produce defects in mitochondria function by decreasing respiratory capacity (Fig. 2-2 F-G), suggesting that ADO-mediated taurine synthesis is essential for healthy mitochondrial function.

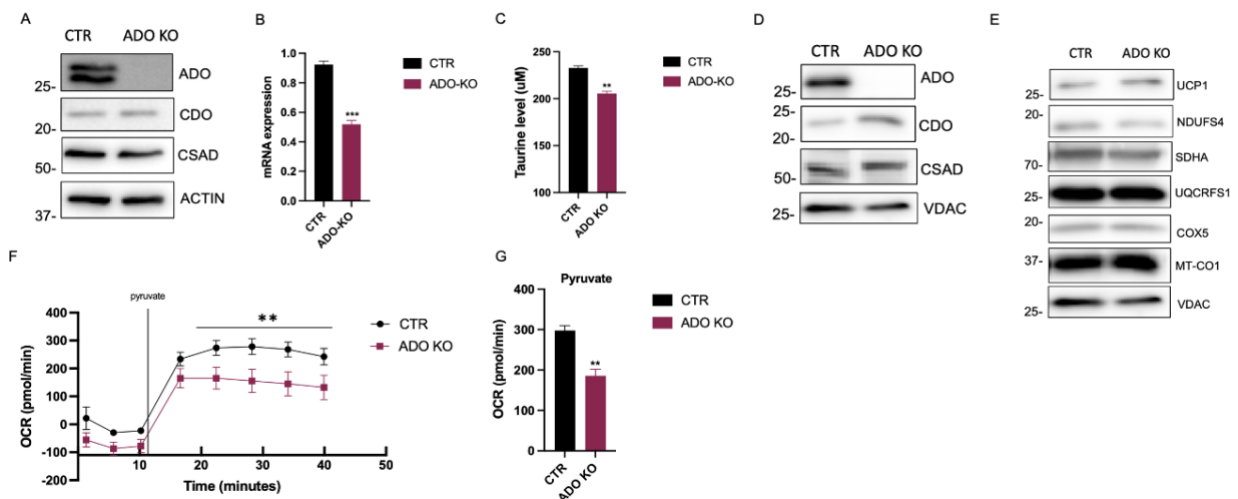


**Figure 2-2 ADO ablation causes defects in mitochondrial metabolism and taurine biosynthesis.**

- (A) Representative immunoblotting of DE control and knock-out cells  
 (B) Relative mRNA expression of DE control and knock-out cells (n=3)  
 (C) Taurine level of DE control and knock-out cells (n=3)  
 (D) Representative immunoblotting of isolated mitochondrial DE control and knock-out cells  
 (E) Representative immunoblotting of UCP-1 and various electron transport chain complexes from isolated mitochondria  
 (F) Oxygen consumption rate of mitochondria extracted from DE control and knock-out cells treated with pyruvate/ malate (n=8)  
 (G) Quantification of pyruvate/ malate-treated oxygen consumption rate of DE control and knock-out cells (n=8).

All figures and data are represented as mean  $\pm$  SEM. \*p < 0.05, \*\*p < 0.01, \*\*\*p < 0.001 by Student's t test.

## CHAPTER 3

### **Aim 2: Quantify the level and localization of taurine in inguinal adipocytes in response to NST activation.**

#### **Research Rationale**

Our previous results demonstrated the taurine biosynthetic enzyme ADO is elevated robustly in inguinal tissues in response to thermogenesis. However, the regulation dynamics of taurine synthesis in thermogenic adipocytes is still enigmatic. In addition, taurine is an ubiquitous sulfur-containing amino acid present in many tissues. In this aim, I will define the taurine localization in the inguinal adipocytes to determine if taurine is retained in the cell, or if it is secreted into circulation to travel to other organs in order to participate in other biological pathways. To address this knowledge gap, my first focus of Aim 2 is to examine the levels of taurine accumulation in the inguinal adipocytes under pharmacologically-induced thermogenesis relative to other cellular metabolites. My second focus of Aim 2 is to trace the localization of taurine in inguinal adipocytes by supplementing the primary inguinal cells with cysteamine at different time points and quantify the amount of taurine both from cells and the media via liquid chromatography–mass spectrometry (LC-MS).

#### **Experiment Model and Methods**

##### **Mouse Primary Inguinal Adipocytes Culture and Differentiation**

For *in vitro* studies, inguinal adipose tissues were harvested from three-week-old male wild-type C57BL/6J mice. Inguinal tissues were minced with scissors thoroughly for 5 minutes and digested by 15 ml of lysis buffer (PBS, 1.3 mM CaCl<sub>2</sub>, 2.4 unit/ml dispase II (Sigma D4693), and 1.5 unit/ml collagenase D) for 15 minutes at 37°C. Suspended cells were filtered through a 100 µm cell strainer and centrifuged for 5 minutes at 600 g at 4°C. The digestion buffer was then removed and the stromal vascular fraction (SVF) was subsequently resuspended in adipocyte culture media (DMEM/F12 with 10% FBS, 25mM HEPES, and 1% PenStrep) and filtered through a 40 µm cell strainer, followed by spinning for 5 minutes at 600 g at 4 °C. After removing the washing media, resuspended the cells with adipocyte culture media, and plated them on coated 10 cm polystyrene cell culture dishes, coated with gelatin. After two days, washed the debris with PBS two times then seeded preadipocytes on culture plates, coated with gelatin. Differentiated the preadipocytes with DMEM/F12 (supplemented with 5 ug/mL insulin, 1 µM Rosiglitazone, 1 µM Dexamethasone, 0.5 mM Isobutylmethylxanthine, and 1 nM T3) until it was post confluency. After 48 hours, the media was replaced with maintenance media (5 ug/mL Insulin and 1 µM Rosiglitazone). The medium was replenished every two days until Day 7 for different drug treatments, as demonstrated below.

## **Metabolomics**

For *in vivo* studies, six-week-old mice were injected daily via intraperitoneal injection (IP) with saline or with 1 mg/kg CL 316,243 (Cayman #17499) (n=5, per treatment) for 7 days. During harvesting, mice were euthanized with carbon dioxide and inguinal adipocytes were collected, followed by biphasic extraction. For *in vitro* studies, after primary inguinal cells were fully differentiated, they were separately treated with DMSO, 1  $\mu$ M CL (Cayman #17499), and 1mM cysteamine (Cayman #33297) at different time points (24 hours and 30 minutes, n=3). Subsequently, cells and media were processed by biphasic extraction, and the taurine level was measured via LC-MS, conducted by the Harvard Center for Mass Spectrometry.

## **Biphasic Extraction**

For *in vivo* studies, inguinal tissues had been homogenized by metal beads with 2 mL cold methanol, followed by mixing with 4 mL of cold chloroform. For *in vitro* studies, the primary inguinal cells had been scrapped with 1.6 mL cold methanol and mixed with 400  $\mu$ L of internal standard, 2  $\mu$ M taurine (13C2, 99%; 15N, 98%, Cambridge isotope #CNLM-10253-PK), as well as 4 mL cold chloroform. After vortexing for one minute, 2 mL of molecular grade water were added and mixed. After incubation for 5 minutes, samples were centrifuged at 4  $^{\circ}$ C for 10 min at 3000 g, then transferred 3 mL supernatant to 15 mL conical tubes and stored at -80  $^{\circ}$ C.

## **Quantification and Statistical Analysis**

All data were expressed as mean  $\pm$  SEM unless otherwise annotated. Two-tailed unpaired Student's t-test and multiple t-tests were performed to determine the difference between the two independent groups. GraphPad Prism 9 was used for statistical analysis. Comparison of LC-MS data was calculated by analysis of variance (ANOVA), followed by Tukey's HSD post hoc test, performed by the software Compound Discoverer 3.2 (Thermo Fisher). The significance level was considered at  $p < 0.05$ . The value of n and the statistical parameters are illustrated in each figure legend.

## **Results**

**NST activation resulted in intracellular taurine accumulation in inguinal adipocytes.** To assess the taurine level under pharmacologically-activated thermogenesis, we supplemented primary inguinal cells with CL 316, 243 for 24 hours. The taurine level robustly increased in response to adrenergic signals (Fig. 3A) which was consistent with our previous data, demonstrating that thermogenesis can increase taurine biosynthetic enzymes in inguinal tissues (Fig. 2-2E). While it has been demonstrated that taurine levels may rise under thermogenic conditions, academic studies have yet to comprehend the dynamic localization of taurine in the inguinal tissues. Therefore, to gain a full understanding of how metabolites change in response to adrenergic signals we performed untargeted metabolomics to compare the difference between control and CL 316, 243. To understand the systematic metabolic alteration under pharmacologically-activated thermogenesis, we conducted an animal study by injecting mice with the  $\beta$ 3 receptor agonist CL 316, 243 for seven days. This led to an increase in taurine levels as observed previously but surprisingly, the accumulation of taurine was modest compared to the other cellular metabolites (Fig. 3B). We hypothesized that the amount of endogenous taurine under thermogenetic stimulation after 7 days was modest because perhaps, we missed the earlier time points of taurine accumulation. Therefore, to accurately assess the dynamic changes of taurine in IGW under thermogenesis, we treated primary inguinal cells with cysteamine accompanied by CL 316, 243 at different time points to measure hypotaurine and taurine synthesis resulting from the ADO-dependent pathway (Fig. 3C). Consistent with the literature illustrating that treating the adipocyte with cysteamine can stimulate hypotaurine and taurine synthesis<sup>30</sup>, when we supplemented the primary inguinal cells with the cysteamine, the ADO protein expression was upregulated in the cysteamine group compared with the control (Fig. 3D). It suggested that the cells can uptake the cysteamine and was catalyzed by ADO to synthesize hypotaurine and subsequently taurine. We then performed targeted metabolomics to measure the intracellular and extracellular taurine and hypotaurine levels to determine the dynamics and localization of taurine accumulation in response to NST. The intracellular hypotaurine levels increased following cysteamine treatment but we did not observe any significant changes at the extracellular level. This demonstrated that the elevated hypotaurine in the inguinal cells accumulated in the adipocytes, and the ADO enzyme activity was stimulated by cysteamine treatment, which was consistent with the upregulated ADO protein expression (Fig. 3E). Surprisingly, intracellular taurine levels did not follow this same pattern with cysteamine supplementation. Taurine levels instead was reduced at both the 30min and 24-hour timepoints. It is possible that the synthesized taurine was rapidly degraded or the hypotaurine was contributed to other metabolic pathways (Fig. 3F). There was no increase in taurine levels in the media indicating that taurine is likely not secreted in inguinal adipocytes. Together, our results suggest that

pharmacologically-activated thermogenesis can increase intracellular hypotaurine and taurine levels and that these metabolites are retained in the cell and not secreted into the extracellular media.

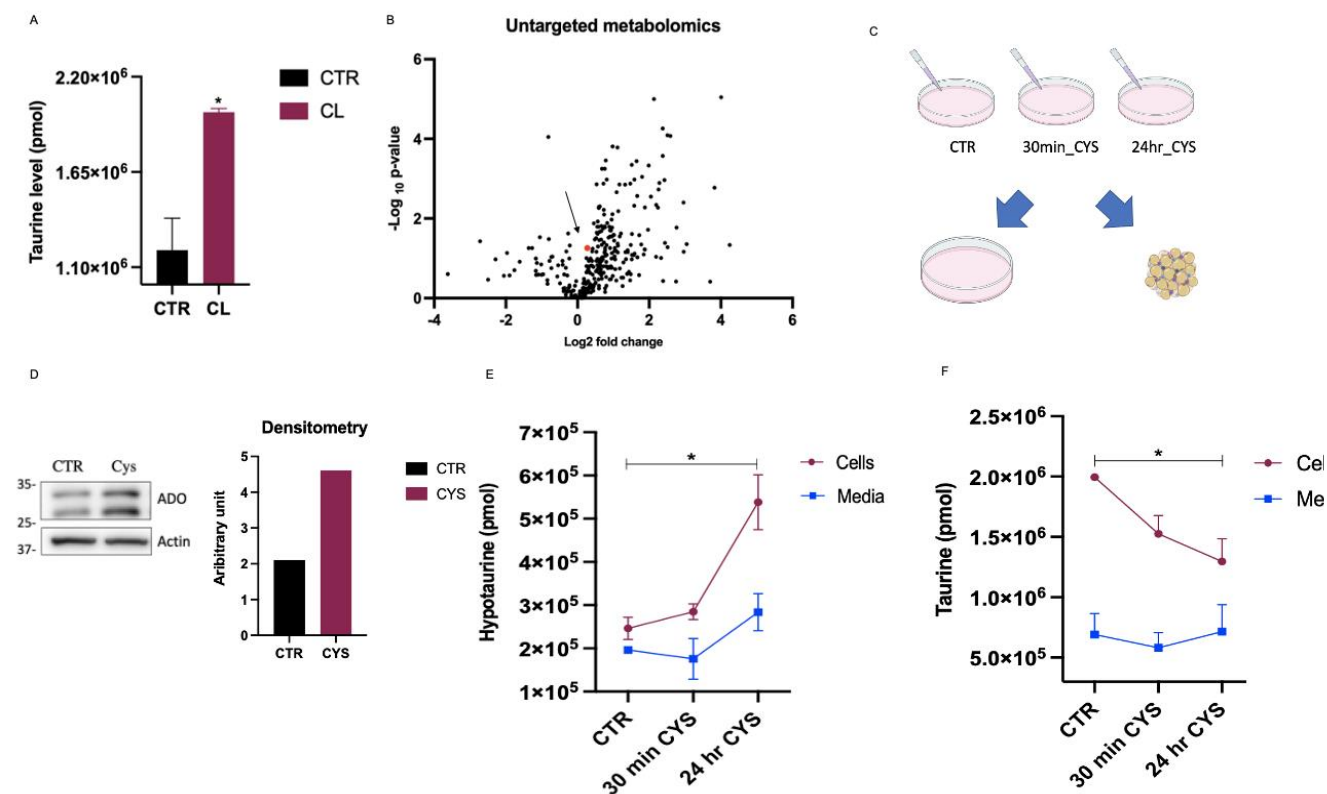


**Figure 3 The elevated taurine levels in response to NST localize in the thermogenic adipocytes.**

- (A) Primary inguinal cells were supplemented with saline or CL for 24 hours. The taurine level was quantified by LC-MS (n=3).
- (B) Volcano plot of metabolites in IGW tissues administrated with saline or CL for 7 days. The log 2-fold change was calculated by the ratio of CL versus saline groups. The -log P-value was analyzed by the multiple t-test adjusted by the FDR method. Red dot represented the taurine expression.
- (C) The scheme of the metabolomic experiment. Primary inguinal cells were treated with CL for 24 hours. Within the cysteamine as subgroups, primary inguinal cells were treated with cysteamine in different time points. The hypotaurine and taurine level in the primary IGW cells or media were analyzed and quantified by LC-MS.
- (D) Immunoblotting of ADO expression in primary inguinal cells supplemented with PBS or cysteamine for 24 hours (left). Protein quantification level of ADO in primary inguinal cells (right).
- (E) Hypotaurine level in the cells (purple) or media (blue) analyzed and quantified by LC-MS.
- (F) Taurine level in the cells (purple) or media (blue) were analyzed and quantified by LC-MS.
- All figures and data are represented as mean ± SEM. \*p < 0.05, \*\*p < 0.01, \*\*\*p < 0.001 by Student's t test or multiple t test.

## CHAPTER 4

### **Aim: Assess the impact of taurine on chromatin accessibility in thermogenic adipocytes**

#### **Research Rationale**

Our previous results demonstrated that pharmacologically-activated thermogenesis can increase taurine biosynthetic enzyme expression and can elevate taurine levels that are retained in the inguinal adipocytes. The role of taurine in the inguinal adipocyte however is unknown. We hypothesized that the taurine accumulation in the inguinal adipocytes may have the ability to contribute to thermogenic activation. According to the literature, mice treated with the taurine resulted in the elevation of thermogenic markers such as UCP-1 and PGC1-alpha in the inguinal tissues<sup>32</sup>. However, it is not known how taurine mediates the increase of these thermogenic markers and whether the effect is mediated at the gene, transcript, or protein level. We hypothesize that taurine plays a role in modulating chromatin structure to make thermogenic genes more accessible for transcription. We will be the first to define whether taurine has the ability to modulate chromatin structure in inguinal adipocytes. Therefore, to analyze the large-scale linkage of taurine and thermogenesis at the chromatin level, the focus of my Aim 3 is to profile the chromatin accessibility of the primary inguinal cells supplemented with taurine and perform the Assay for Transposase-Accessible Chromatin using sequencing (ATAC-seq). The results from the ATAC-seq will allow us to define global genomic regions in the chromatin in response to taurine supplementation.

#### **Experiment Model and Methods**

##### **Nuclei Extraction and ATAC-seq analysis**

Primary inguinal cells, plated on 10 cm culture plates, were washed with cold PBS and scrapped with 1mL PBS. Samples were centrifuged at 4 °C for 10 min at 200 g to pellet the cells. Cell pellets were resuspended with 200 uL lysis buffer (10 mM Tris-HCl (pH 7.4), 10mM NaCl, 3mM MgCl<sub>2</sub>, 0.1% Tween-20, 0.1% Nonidet P40 Substitute, 0.01% Digitonin, and 1% BSA) and processed by plastic-Teflon homogenizer for one minute. After several pipetting and incubation, the total volume of samples was brought to 2 mL with washing buffer (10 mM Tris-HCl (pH 7.4), 10mM NaCl, 3mM MgCl<sub>2</sub>, 0.1% Tween-20, 0.1%, and 1% BSA) and spun down at 4 °C for 10 min at 500 g. the supernatant was removed and the cell pellets were homogenized by the plastic-Teflon in 300 uL washing buffer, followed by filtering the samples through 70 um nylon filter. Subsequently, samples were centrifuged at 4 °C for 10 min at 500 g for three times, and then cell pellets were resuspended with transposition mix TD buffer, and filtered through 40 um nylon filter. For nuclei quantification, the samples were treated with DAPI (4, 6-diamidino-2-phenylindole) and trypan blue in a 1:1:2 ratio.

Incubation of transposition reactions was then performed at 37 °C for 30 min while shaking at 1,000 r.p.m in a thermomixer. Reactions were cleaned up with DNA columns, and the samples were followed by a PCR reaction to amplify the DNA. For library size distribution profiling, the samples were analyzed by the Cornell University Core Facility. After confirming the typical nucleosome patterns, samples were sequenced at the Cornell University Core Facility. The library preparation and statistical analysis have collaborated with Dr. Soloway's lab. The ATAC-seq signal peaks were performed by the Integrated Genome Browser.

### **Gene Ontology Analysis**

Gene ontology analysis (GO) was performed using Shiny GO v0.741 on selected top 50 downregulated and upregulated gene accessibilities that p-value was less than 0.05. Bar graph illustrating the top 10 GO terms for biological process was illustrated by GraphPad Prism 9.

## **Results**

**Taurine increases the chromatin accessibility of hypoxia-inducible signaling and glucose metabolism genes.** To define the biological impact of taurine in primary inguinal cells, we performed a genome-wide analysis using ATAC-seq to discover the association between taurine and thermogenic adipocytes chromatin accessibility. We began by supplementing the primary inguinal cells with 1mM taurine for 24 hours to induce chromatin alteration. Subsequently, we isolated the genomic DNA from the extracted inguinal nuclei for ATAC-seq analysis (Figure 4A). Next, to capture the global impact of taurine administration on chromatin structure and accessibility, we compared the global differential gene accessibilities between taurine treated inguinal cells to vehicle controls. As demonstrated by the volcano plot, the taurine supplementation identified significantly differential chromatin accessibility patterns in multiple gene loci (Figure 4B). While it is clear from the volcano plot that taurine can alter the chromatin accessibility of inguinal cells, the functional classification of those genes needed to be defined. Therefore, to discover their biological processes, we performed gene ontology analyses (GO). We anticipated seeing strong chromatin accessibility changes in thermogenic genes but unfortunately taurine treatment only modestly altered accessibility of the thermogenic pathway. We did however observe major gene enrichments accessibility associated with genes in the hypoxia-inducible factor 1 (HIF-1) signaling pathway and glucose catabolic metabolism (Figure 4C, Figure S1A). Furthermore, among the top upregulated differential gene accessibilities, the gene implicated in hypoxia-mediated mitophagy by removing unfunctional mitochondria, Bnip3 (BCL2 Interacting Protein 3), displayed increased chromatin accessibility when taurine was supplemented to primary inguinal cells, suggesting that taurine may regulate this gene (Figure 4D). In addition, taurine also silenced the chromatin accessibility of certain genes such as Thbs1 (Thrombospondin 1), which has a positive correlation with metabolic disease and obesity (Figure 4E). In future studies, it will be interesting to further define if the chromatin accessibility changes also correlate with gene activity and function. In summary, we were able to demonstrate that the amino acid taurine has the ability to alter chromatin accessibility in primary inguinal cells. Taurine treatment enriched the chromatin accessibility of genes in the hypoxia-inducible pathway and glycolytic processes may link the hypoxia-mediated mitochondrial functions and the glucose metabolism, which could serve as substrate to drive the thermogenic process<sup>27</sup> to characterize the potential role of taurine in alleviating obesity and metabolic disease.

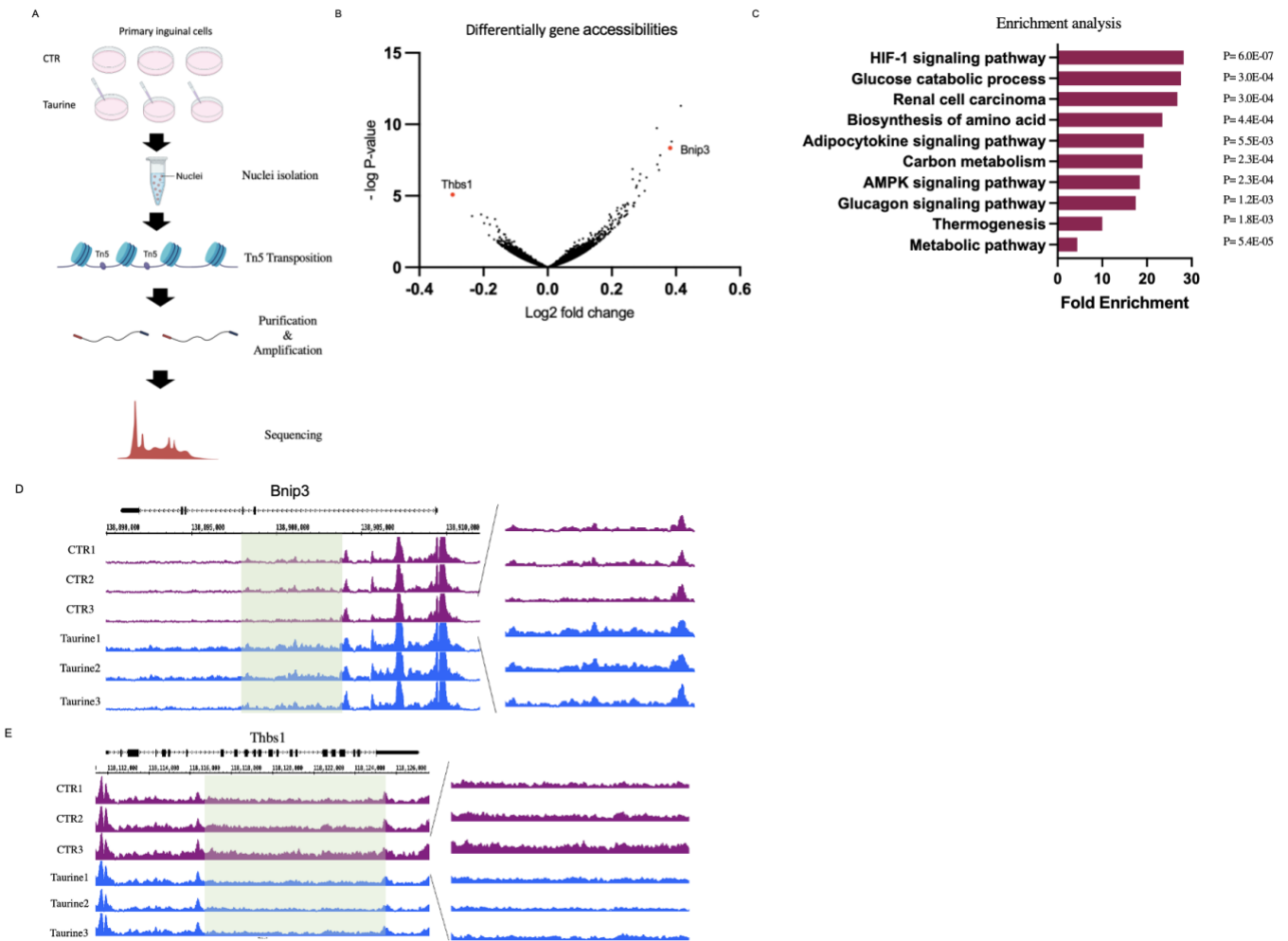


**Figure 4. Chromatin accessibility profiling in primary inguinal cells treated with taurine**

(A) The schematic of ATAC-seq experiment and analysis

(B) Volcano plot showing the differentially gene accessibilities between taurine versus control in primary inguinal adipocytes

(C) GO enrichment analysis of differentially gene accessibilities between taurine and control groups

(D-E) Genome browser view of ATAC-seq signal for the indicated upregulated gene, *Bnip3* and downregulated gene *Thbs1*.

## Chapter 5

### **Discussion**

Obesity is a national epidemic, but current treatment options are often ineffective for long-term weight loss and have serious side effects. One of the molecular approaches, non-shivering thermogenesis (NST), has been recognized as one potential method to combat this health issue. While the activation effect of environmental stimulus and pharmacological treatments on NST is well-studied, there are still no safe and realistic approaches to activate NST in humans to prevent obesity. Interestingly, current studies have documented that taurine has the ability to prevent diet-induced obesity. However, no studies have directly identified how taurine mediates this effect.

As a result of the thermogenic activation, we observed significant upregulation of the taurine biosynthetic enzyme, ADO (Fig. 2-1H). Following the protein expression, the endogenous taurine levels derived from primary inguinal cells also increased with adrenergic stimulation (Fig 3A). Therefore, we hypothesized that the taurine biosynthesis stimulated by the NST is dominantly from the ADO-dependent pathway. We knocked out ADO in the thermogenic adipose cell line to examine whether taurine biosynthesis would be affected by ADO ablation and lead to defects in thermogenesis. Notably, the taurine level decreased significantly in the ADO-KO and the loss of taurine also blunted the mitochondrial oxygen consumption rate (OCR) (Figure 2-2 C, F). However, ablation of ADO still had 80% of taurine left, so we considered that the taurine biosynthesis might be compensated by the CDO and CSAD enzyme activity in the ADO-KO. Otherwise, the decreased level of taurine might be more obvious in the inguinal ADO-KO cell line. Collectively, the loss of function model demonstrated that ADO is essential for taurine synthesis, and the taurine plays a crucial role in maintaining healthy mitochondria function.

Taurine is one of the most abundant free amino acids in mammals, but this metabolite seems like the end product in the metabolic pathway. One physiological documented function of taurine is its conjugation with bile acids to regulate lipid metabolism which occurs in the liver<sup>37</sup>. This would suggest that taurine is perhaps synthesized in the inguinal tissue and will be secreted into circulation so it can travel to the liver. We performed targeted metabolomics to examine the dynamic localization of taurine in primary inguinal cells to determine whether taurine produced by thermogenic adipocytes would be secreted or retained in the cells. Consistent with the literature<sup>30</sup>, we observed that primary inguinal cells supplemented with the cysteamine, the ADO substrate, significantly increased the expression of ADO proteins and enzyme activity, as demonstrated by the increased level of intracellular hypotaurine

(Fig 3D-E). To our surprise, the upregulated level of hypotaurine did not relatively convert into taurine synthesis. Thus, we hypothesized that the inconsistent conversion might relate to the catalyzing activity of the hypotaurine dehydrogenase or the accumulated hypotaurine contributing differently. Current studies have not identified the oxygenized step of hypotaurine to taurine, yet some novel research has demonstrated that hypotaurine can be oxidized by flavin-containing monooxygenases (FMOs) rather than the hypotaurine dehydrogenase to produce taurine<sup>38,39</sup>. According to all current research, while the hypotaurine catalyzing enzyme is still debatable, the established metabolic direction of hypotaurine is only contribute to taurine synthesis. Therefore, we suggest that the decreased level of taurine in the cysteamine supplementation group might not because the hypotaurine contributes to other pathways or the hypotaurine would not be able to catalyze to produce taurine. Thus, we suggest the decreased level of taurine might result from the rapid depletion of taurine in the inguinal cells, or related to the substrate inhibition effect. In short, based on no significant change in extracellular hypotaurine and taurine levels in the primary inguinal cells, we concluded that the elevated intracellular taurine level in the inguinal adipocytes in responses to thermogenesis would localize in the depots without secretion.

While we only detected a modest change of taurine in the inguinal tissues under pharmacologically-activated thermogenesis, the downregulated taurine levels in the ADO-KO did impede the healthy mitochondrial function in thermogenic adipocytes (Fig 2-2 F) indicating that taurine plays an essential functional role in inguinal adipocytes. Therefore, to discover what that role could be, we performed ATAC-seq to analyze if taurine can modulate chromatin structure that defines the potential mechanism of how taurine impact thermogenic adipocytes to prevent obesity. According to our results, taurine supplementation did alter the chromatin biology of thermogenic adipocytes (Fig 4C). However, the most significant gene enrichment accessibility was strongly associated with the hypoxia-inducible factor 1 (HIF-1) signaling pathway and glucose catabolic metabolism. Interestingly, one study has shown that ablation of HIF factors can cause lipid accumulation and inflammation in brown adipocytes<sup>40</sup>. One of the hypoxia-inducible signaling factors is known as Bnip3<sup>41</sup>, which has been reported as an activator that can regulate mitochondrial turnover by activating mitochondrial autophagy<sup>42-44</sup>. The chromatin accessibility profiling demonstrated enrichments in the Bnip3 and other hypoxia-inducible factors, suggesting that taurine would affect the mitochondrial function to drive the thermogenic process. In addition, we also identified that taurine supplementation can silence the chromatin structure in Thbs1. Thbs1 is highly expressed in adipocytes, which can be induced by a high-fat diet (HFD) and is positively correlated with obesity<sup>45</sup>. One study has illustrated that knocking out of Thbs1 in mice can rescue the insulin resistance induced by HFD<sup>46</sup>, it demonstrates that taurine might have the ability to prevent diet-induced obesity. As a whole, our results illustrate that

thermogenic signals make the taurine localize in the inguinal adipocytes and that the accumulated levels of intracellular taurine can influence the chromatin structure by increasing the accessibilities of genes involved in the regulation of healthy mitochondrial function and thermogenic-driven metabolism or silence the metabolic disorder-inducible gene. In the future, it will be interesting to test whether the alteration of chromatin biology induced by taurine can transcribe into protein expression and illustrate the potential molecular role of taurine in preventing obesity and metabolic diseases.

## Chapter 6

### References

1. Allison, D. B., Fontaine, K. R., Manson, J. E., Stevens, J. & Vanitallie, T. B. *Annual Deaths Attributable to Obesity in the United States*. <https://jamanetwork.com/>.
2. Finkelstein, E. A., Trogdon, J. G., Cohen, J. W. & Dietz, W. Annual Medical Spending Attributable To Obesity: Payer-And Service-Specific Estimates. *Health Affairs* **28**, (2009).
3. Tartof, S. Y. *et al.* Obesity and Mortality Among Patients Diagnosed With COVID-19: Results From an Integrated Health Care Organization. *Annals of Internal Medicine* **173**, (2020).
4. King, W. C., Hinerman, A. S., Belle, S. H., Wahed, A. S. & Courcoulas, A. P. Comparison of the Performance of Common Measures of Weight Regain After Bariatric Surgery for Association With Clinical Outcomes. *JAMA* **320**, (2018).
5. Stroh, C. *et al.* Results of More Than 11,800 Sleeve Gastrectomies. *Annals of Surgery* **263**, (2016).
6. Leitner, B. P. *et al.* Mapping of human brown adipose tissue in lean and obese young men. *Proceedings of the National Academy of Sciences* **114**, (2017).
7. Steiner, G., Loveland, M. & Schonbaum, E. Effect of denervation on brown adipose tissue metabolism. *American Journal of Physiology-Legacy Content* **218**, (1970).
8. van Marken Lichtenbelt, W. D. *et al.* Cold-Activated Brown Adipose Tissue in Healthy Men. *New England Journal of Medicine* **360**, (2009).
9. Golozoubova, V., Cannon, B. & Nedergaard, J. UCP1 is essential for adaptive adrenergic nonshivering thermogenesis. *American Journal of Physiology-Endocrinology and Metabolism* **291**, (2006).
10. Enerbäck, S. *et al.* Mice lacking mitochondrial uncoupling protein are cold-sensitive but not obese. *Nature* **387**, (1997).
11. Lee, P. *et al.* Temperature-Acclimated Brown Adipose Tissue Modulates Insulin Sensitivity in Humans. *Diabetes* **63**, (2014).
12. Xiao, C., Goldgof, M., Gavrilova, O. & Reitman, M. L. Anti-obesity and metabolic efficacy of the  $\beta$ 3-adrenergic agonist, CL316243, in mice at thermoneutrality compared to 22°C. *Obesity* **23**, (2015).
13. Kim, J. *et al.* Regulation of Brown and White Adipocyte Transcriptome by the Transcriptional Coactivator NT-PGC-1 $\alpha$ . *PLOS ONE* **11**, (2016).
14. Keipert, S. & Jastroch, M. Brite/beige fat and UCP1 — is it thermogenesis? *Biochimica et Biophysica Acta (BBA) - Bioenergetics* **1837**, (2014).
15. Petrovic, N. *et al.* Chronic Peroxisome Proliferator-activated Receptor  $\gamma$  (PPAR $\gamma$ ) Activation of Epididymally Derived White Adipocyte Cultures Reveals a Population of Thermogenically Competent, UCP1-containing Adipocytes Molecularly Distinct from Classic Brown Adipocytes. *Journal of Biological Chemistry* **285**, (2010).
16. Huxtable, R. J. Physiological actions of taurine. *Physiological Reviews* **72**, 101–163 (1992).
17. Maleki, V., Alizadeh, M., Esmaeili, F. & Mahdavi, R. The effects of taurine supplementation on glycemic control and serum lipid profile in patients with type 2 diabetes: a randomized, double-blind, placebo-controlled trial. *Amino Acids* **52**, (2020).

18. da Silva, L. A. *et al.* Effects of taurine supplementation following eccentric exercise in young adults. *Applied Physiology, Nutrition, and Metabolism* **39**, (2014).
19. Balshaw, T. G., Bampouras, T. M., Barry, T. J. & Sparks, S. A. The effect of acute taurine ingestion on 3-km running performance in trained middle-distance runners. *Amino Acids* **44**, (2013).
20. Suzuki, T., Suzuki, T., Wada, T., Saigo, K. & Watanabe, K. Taurine as a constituent of mitochondrial tRNAs: new insights into the functions of taurine and human mitochondrial diseases. *EMBO J* **21**, 6581–9 (2002).
21. Zhang, M. *et al.* Beneficial effects of taurine on serum lipids in overweight or obese non-diabetic subjects. *Amino Acids* **26**, (2004).
22. Kim, K. S., Doss, H. M., Kim, H.-J. & Yang, H.-I. Taurine Stimulates Thermoregulatory Genes in Brown Fat Tissue and Muscle without an Influence on Inguinal White Fat Tissue in a High-Fat Diet-Induced Obese Mouse Model. *Foods* **9**, (2020).
23. Rosa, F. T., Freitas, E. C., Deminice, R., Jordão, A. A. & Marchini, J. S. Oxidative stress and inflammation in obesity after taurine supplementation: a double-blind, placebo-controlled study. *European Journal of Nutrition* **53**, (2014).
24. Murakami, S. The physiological and pathophysiological roles of taurine in adipose tissue in relation to obesity. *Life Sciences* **186**, (2017).
25. Learn, D. B., Fried, V. A. & Thomas, E. L. Taurine and Hypotaurine Content of Human Leukocytes. *Journal of Leukocyte Biology* **48**, (1990).
26. Guo, Y.-Y., Li, B.-Y., Peng, W.-Q., Guo, L. & Tang, Q.-Q. Taurine-mediated browning of white adipose tissue is involved in its anti-obesity effect in mice. *Journal of Biological Chemistry* **294**, (2019).
27. Panic, V. *et al.* Mitochondrial pyruvate carrier is required for optimal brown fat thermogenesis. *Elife* **9**, (2020).
28. Fujimoto, Y. *et al.* Metabolic changes in adipose tissues in response to  $\beta_3$ -adrenergic receptor activation in mice. *Journal of Cellular Biochemistry* **120**, (2019).
29. Kim, K. S. *et al.* Anti-obesity effect of taurine through inhibition of adipogenesis in white fat tissue but not in brown fat tissue in a high-fat diet-induced obese mouse model. *Amino Acids* **51**, (2019).
30. Ueki, I. & Stipanuk, M. H. Enzymes of the Taurine Biosynthetic Pathway Are Expressed in Rat Mammary Gland. *The Journal of Nutrition* **137**, (2007).
31. Ueki, I. & Stipanuk, M. H. 3T3-L1 Adipocytes and Rat Adipose Tissue Have a High Capacity for Taurine Synthesis by the Cysteine Dioxygenase/Cysteinesulfinatase Decarboxylase and Cysteamine Dioxygenase Pathways. *The Journal of Nutrition* **139**, (2009).
32. Dominy, J. E. *et al.* Discovery and Characterization of a Second Mammalian Thiol Dioxygenase, Cysteamine Dioxygenase. *Journal of Biological Chemistry* **282**, (2007).
33. Stipanuk, M. H., Simmons, C. R., Andrew Karplus, P. & Dominy, J. E. Thiol dioxygenases: unique families of cupin proteins. *Amino Acids* **41**, (2011).
34. Lombardini J.B., T. P. , B. D. R. & S. T. P. Cysteine oxygenase: 1. General properties. *Physiol. Chem. & Physics* 1–23 (1969).
35. Cavallini, D., de Marco, C., Scandurra, R., Dupré, S. & Graziani, M. T. The enzymatic oxidation of cysteamine to hypotaurine. Purification and properties of the enzyme. *J Biol Chem* **241**, (1966).

36. Tsuboyama-Kasaoka, N. *et al.* Taurine (2-Aminoethanesulfonic Acid) Deficiency Creates a Vicious Circle Promoting Obesity. *Endocrinology* **147**, (2006).
37. Yanagita, T. *et al.* Taurine reduces the secretion of apolipoprotein B100 and lipids in HepG2 cells. *Lipids in Health and Disease* **7**, 38 (2008).
38. Veeravalli, S. *et al.* Flavin-Containing Monooxygenase 1 Catalyzes the Production of Taurine from Hypotaurine. *Drug Metabolism and Disposition* **48**, 378–385 (2020).
39. Huang, S., Howington, M. B., Dobry, C. J., Evans, C. R. & Leiser, S. F. Flavin-Containing Monooxygenases Are Conserved Regulators of Stress Resistance and Metabolism. *Frontiers in Cell and Developmental Biology* **9**, (2021).
40. García-Martín, R. *et al.* Adipocyte-Specific Hypoxia-Inducible Factor 2 $\alpha$  Deficiency Exacerbates Obesity-Induced Brown Adipose Tissue Dysfunction and Metabolic Dysregulation. *Molecular and Cellular Biology* **36**, 376–393 (2016).
41. Gustafsson, Å. B. Bnip3 as a Dual Regulator of Mitochondrial Turnover and Cell Death in the Myocardium. *Pediatric Cardiology* **32**, 267–274 (2011).
42. Rikka, S. *et al.* Bnip3 impairs mitochondrial bioenergetics and stimulates mitochondrial turnover. *Cell Death & Differentiation* **18**, 721–731 (2011).
43. Gao, A., Jiang, J., Xie, F. & Chen, L. Bnip3 in mitophagy: Novel insights and potential therapeutic target for diseases of secondary mitochondrial dysfunction. *Clinica Chimica Acta* **506**, 72–83 (2020).
44. Choi, J. W. *et al.* BNIP3 is essential for mitochondrial bioenergetics during adipocyte remodelling in mice. *Diabetologia* **59**, 571–581 (2016).
45. Varma, V. *et al.* Thrombospondin-1 Is an Adipokine Associated With Obesity, Adipose Inflammation, and Insulin Resistance. *Diabetes* **57**, 432–439 (2008).
46. Inoue, M. *et al.* Thrombospondin 1 Mediates High-Fat Diet-Induced Muscle Fibrosis and Insulin Resistance in Male Mice. *Endocrinology* **154**, 4548–4559 (2013).

## Chapter 7

### Supplementary Data

Pathway Description	Gene
Hypoxia related genes	Fam162a, Ndr1, Cox4i2, Ddit4, Vegfa, Ak4, Slc2a1, Egl1, Plod2, Egl3, Ccl2, Pdk1, Bnip3
Glucose metabolism related genes	Pfkfb3, Pfkfb1, Gpi1, Pfkfb2, Gys1, Slc2a1
Renal cell carcinoma related genes	Vegfa, Slc2a1, Egl1, Egl3
Biosynthesis of amino acids related genes	Pfkfb3, Shmt2, Pfkfb1, Pfkfb2
Adipocytokine signaling pathway related genes	Acs1, Slc2a1, Acs4
Carbon metabolism related genes	Pfkfb3, Shmt2, Pfkfb1, Gpi1, Pfkfb2
AMPK signaling pathway related genes	Gys1, Pfkfb3, Ulk1, Ppp2r2d
Glucagon signaling pathway related genes	Gys1, Pfkfb3, Slc2a1, Pfkfb1
Thermogenesis related genes	Cox4i2, Acs1, Acs4, Ndafa412, Kdm3a
Metabolic pathways related genes	Gys1, Cox4i2, Acs1, P4ha1, Pfkfb3, Shmt2, Pfkfb1, Ak4, Acs4, Pfkfb2, Plod2, Gpi1, Ndafa412, Pfkfb2, Selenbp1

S1A: Gene list for different biological pathways demonstrated in figure 4c